

## Capturing Transient Structures in the Elimination Reaction of Haloalkane in Solution by Transient X-ray Diffraction

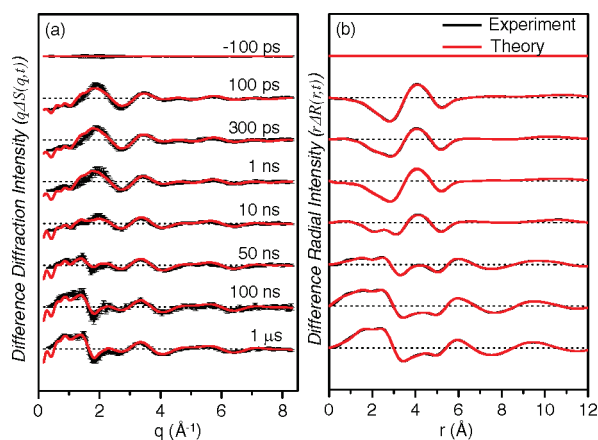
Jae Hyuk Lee,<sup>†</sup> Tae Kyu Kim,<sup>‡</sup> Joonghan Kim,<sup>†</sup> Qingyu Kong,<sup>§</sup> Marco Cammarata,<sup>§</sup> Maciej Lorenc,<sup>§</sup> Michael Wulff,<sup>§</sup> and Hyotcherl Ihee<sup>\*†</sup>

Center for Time-Resolved Diffraction, Department of Chemistry, KAIST, Daejeon 305-701, Korea, Department of Chemistry and Chemistry Institute for Functional Materials, Pusan National University, Busan 609-735, Korea, and European Synchrotron Radiation Facility (ESRF), BP220, Grenoble Cedex 38043, France

Received November 12, 2007; E-mail: hyotcherl.ihee@kaist.ac.kr

Here we report the simultaneous tracking of structural and kinetic information for the photoinduced elimination reaction of 1,2-diiodotetrafluoroethane ( $C_2F_4I_2$ ) in methanol solution using transient X-ray diffraction (TXD).<sup>1</sup> The iodine elimination reaction of  $C_2F_4I_2$  is known to produce a short-lived ( $\cdot CF_2CF_2I$ ) intermediate, which can further dissociate into  $C_2F_4$  and  $I$ .<sup>2</sup> Whether the intermediate is a bridged radical or an open structure, that is, the classical mixture of anti and gauche conformers, is a critical issue for stereochemical control in organic synthesis.<sup>3</sup> The structure of a short-lived  $\cdot CF_2CF_2I$  in the gas phase was determined to be classical form by ultrafast electron diffraction, which is a powerful tool in investigating molecular structures of short-lived intermediates in the gas phase.<sup>4</sup> However, whether classical structures are also energetically favored in solution remained to be revealed. In addition, the solvent may greatly influence the reaction kinetics such as the time constant for secondary C–I bond dissociation.<sup>5</sup> These fundamental questions have remained unanswered. For example, transient absorption spectroscopy in solution phase<sup>2b</sup> could not elucidate the structure of the intermediate(s) and measure the time constant for the secondary dissociation. With its proven ability to study spatiotemporal kinetics in solution,<sup>1a,b</sup> TXD was employed to unravel the structure of the intermediates and their kinetics. Since the transient structure of  $\cdot CH_2CH_2I$  in solution was shown by TXD to be bridged,<sup>1a</sup> a comparative study of  $\cdot CF_2CF_2I$  in solution can directly show the effect of fluorine substitution on the molecular structure of a radical.<sup>3d</sup> However, in solution, the solute is surrounded by solvent molecules and the diffraction signal is more complicated since the signals from the solvent cage and the thermally excited solvent has to be considered, making the data analysis nontrivial.<sup>1a,b</sup> In addition, this molecular system offers a challenge for quantitative analysis because  $C_2F_4I_2$  exists as a mixture of anti and gauche conformers.

Time-resolved X-ray diffraction data were collected on beamline ID09B at the ESRF using a pump–probe scheme.<sup>1a,b</sup> Picosecond laser pulses (2 ps, 267 nm, 50  $\mu J$ /pulse) were used to initiate iodine elimination in  $C_2F_4I_2$ , and delayed X-ray pulses ( $5 \times 10^8$  photons per pulse, 100 ps (fwhm), 3% bandwidth around the wavelength of 0.68 Å, repeated at 986.3 Hz) from the synchrotron were used to interrogate the evolving structures in the sample. The liquid sample was injected into the laser/X-ray beam using a recirculating open jet with 60 mM of  $C_2F_4I_2$  dissolved in methanol. Diffraction data were collected for 10 time-delays from –100 ps up to 1  $\mu s$ , and each delay was interleaved by a measurement at –3 ns, which served as a reference for the unperturbed sample.



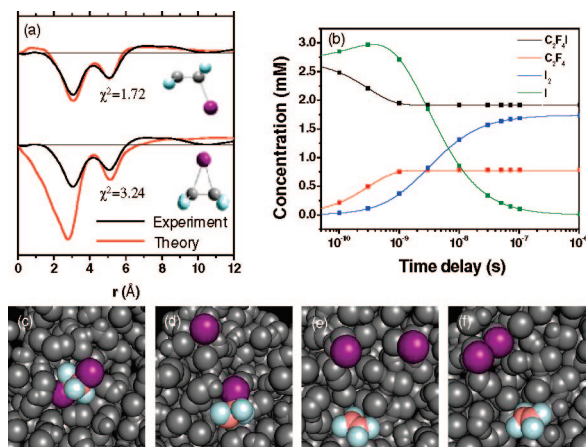
**Figure 1.** Time-resolved X-ray diffraction data at selected time-delays for  $C_2F_4I_2$  in methanol. (a) Difference-diffraction intensities,  $q\Delta S(q,t)$ , excited minus nonexcited (black). Theoretical fits from global-fitting analysis are also shown (red). (b) Difference radial intensities,  $r\Delta R(r,t)$  which are sine-Fourier transforms of  $q\Delta S(q,t)$ .

Figure 1 shows difference diffraction intensities  $q\Delta S(q,t)$ , ( $q = 4\pi/\lambda \sin(\theta)$  where  $\lambda$  is the X-ray wavelength,  $2\theta$  is the scattering angle, and  $t$  the time-delay) and the corresponding radial difference curves,  $r\Delta R(r,t)$ , where  $r$  is the interatomic distance, which is the sine-Fourier transform of  $q\Delta S(q,t)$  at selected time-delays. It is intuitively helpful to examine the Fourier transform whose peaks are a measure of the radial-density-change as seen from the center of an average excited atom.<sup>1c</sup> The broad negative peak at  $\sim 3.0$  Å corresponds to a superposition of depletions of C–I, C $\cdots$ I and F $\cdots$ I interatomic distances and the negative peak at  $\sim 5.0$  Å to the initial I $\cdots$ I interatomic distance in the parent molecule. The positive peak around  $\sim 4.0$  Å is assigned to a reorganization of the solvent around the truncated solute (new cage). However, structure determination in solution requires quantitative analysis of three signals that are mutually constrained by energy conservation in the X-ray illuminated volume. The three components are (i) the solute-only term, (ii) the solute–solvent cross term, and (iii) the solvent-only term from the hydrodynamics; changes in the solvent are mathematically correlated by energy and mass conservation. The first term is due to the change in the internal solute structure which can be described by Debye scattering, that is, the scattering from isolated molecules as in the gas phase.<sup>4a,b</sup> The second term can be simulated by molecular dynamics simulations by considering the interactions between solute–solvent atomic pairs. The last term is due to the temperature and pressure change in the solvent which can be obtained in a separate experiment where the pure solvent is vibrationally excited by near-infrared light.<sup>6</sup> The details of the global-fitting procedure can be found in our previous publications.<sup>1a,b</sup>

<sup>†</sup> KAIST.

<sup>‡</sup> Pusan National University.

<sup>§</sup> European Synchrotron Radiation Facility.



**Figure 2.** (a) Identification of the transient structures of dissociated  $\text{C}_2\text{F}_4\text{I}_2$  in solution at 100 ps by transient X-ray diffraction (TXD). The solute-only terms for the two candidate models (classical and bridged) are shown. The  $\chi^2$  value of the classical structure model is much smaller than that of the bridged showing that the  $\text{C}_2\text{F}_4\text{I}$  radical has the classical structure. (b) Reaction kinetics and population changes of the relevant chemical species during the photoelimination reaction for  $\text{C}_2\text{F}_4\text{I}_2$  in methanol as a function of time. The measured time delays are indicated with symbols. (c–f) Schematic reaction mechanism determined by TXD. (c)  $\text{C}_2\text{F}_4\text{I}_2$  in methanol before laser excitation. (d) Upon photo dissociation, the classical mixtures of  $\text{C}_2\text{F}_4\text{I}$  and iodine atom are formed. (e) Some of the  $\text{C}_2\text{F}_4\text{I}$  intermediate are further dissociated into the  $\text{C}_2\text{F}_4 + \text{I}$  species. (f) After 3 ns, molecular iodine ( $\text{I}_2$ ) is generated by nongeminate recombination.

All putative structures (*anti*-, *gauche*- $\text{C}_2\text{F}_4\text{I}_2$ , *anti*-, *gauche*-, and *bridged*- $\text{C}_2\text{F}_4\text{I}$ ,  $\text{C}_2\text{F}_4$ , and  $\text{I}_2$ ) for the solutes were provided by density functional theory calculations.<sup>7</sup>

According to the previous ultrafast electron diffraction studies in the gas phase,<sup>4a,b</sup> the molecular structure of the  $\text{C}_2\text{F}_4\text{I}$  radical was determined to be classical and not bridged. To unravel its structure in solution, we performed the global-fitting analysis using two candidate models for the transient structures: the *anti*- and *gauche*-mixture (classical structure) and the bridged structure. The  $\chi^2$  value for the fit with the classical model was smaller than that of the bridged structure for all the investigated time-delays. Moreover the  $\chi^2$  value ( $\chi^2 = 1.72$ ) for the classical model was almost a factor of 2 smaller than for the bridged ( $\chi^2 = 3.24$ ) at 100 ps where  $\text{C}_2\text{F}_4\text{I}$  is the major transient chemical species. In addition, when a mixture of the two models is included in the fit, the fraction of bridged radical converges to zero. These findings confirm the formation of the classical mixed structure in the elimination reaction of  $\text{C}_2\text{F}_4\text{I}_2$  in solution. The discrimination in the fits between the classical and bridged forms is enhanced when the solute-only contribution is extracted from the total difference diffraction intensity (Figure 2a). The negative peak near 5 Å corresponding to the  $\text{I}\cdots\text{I}$  interatomic distance in parent  $\text{C}_2\text{F}_4\text{I}_2$  is common in both models, but the broad negative peak between 2.0 and 3.0 Å can only match the classical model. The position and line shape of this peak are indeed very sensitive to the position of the iodine atom relative to the two carbon and four fluorine atoms.

Besides the structural identification of the transient structure, the relative contributions of *anti/gauche* conformers in the  $\text{C}_2\text{F}_4\text{I}$  radical can be obtained from global-fitting analysis. In the global analysis of the TXD data, the fraction of each conformer in the transient molecule was optimized as fitting parameters. The *anti*:*gauche* conformer ratio of the  $\text{C}_2\text{F}_4\text{I}$  radical was determined to be  $86(\pm 4.2):14$ . Figure 2b shows the populations versus time for all the species in the reaction as determined by global-fitting. According to the fit results, the classical- $\text{C}_2\text{F}_4\text{I}$  mixture and  $\text{I}$  dominate at 100 ps as they are essentially created within a few picoseconds. No three-body dissociation to  $\text{C}_2\text{F}_4 + 2\text{I}$  is

observed in the investigated time-regime. Then  $20 \pm 1.3\%$  of the transient classical  $\text{C}_2\text{F}_4\text{I}$  radical decays further into  $\text{C}_2\text{F}_4 + \text{I}$  in picoseconds with the time constant of  $153 \pm 24$  ps. These values can be compared with  $55 \pm 5\%$  and  $26 \pm 7$  ps determined from gas-phase ultrafast electron diffraction,<sup>4a</sup> showing that the solvent reduce the rate and yield of secondary dissociation significantly. These results might be assigned to intermolecular energy transfer to the solvent which typically occurs on a time scale of several tens of picoseconds.<sup>5</sup> Subsequently molecular iodine  $\text{I}_2$  is formed by recombination of two  $\text{I}$  atoms which takes about 100 ns as shown in Figure 2b. The time constant for the formation of  $\text{I}_2$  molecules is  $8.8 (\pm 2.5) \times 10^{10} \text{ M}^{-1} \text{ s}^{-1}$ , which is comparable to the value of the nongeminate recombination of iodine atoms in  $\text{CCl}_4$  from optical spectroscopy.<sup>8</sup>

The time constant for the secondary dissociation obtained in this study relies on a rather small number of measured time delays. To estimate the associated error, we generated mock diffraction data with various time constants (from 50 to 500 ps in steps of 25 ps) for the secondary dissociation. The same analysis applied to the real experimental data was used to fit the time constant out of the mock data, and the fitted time constants agree with the true time constants of the mock data within  $\pm 2$  ps accuracy when no noise was added. If we add noise comparable to experimental noise, then the time constants from the global fit analysis deviate from the true values with a standard deviation of 20 ps. We also note that the convolution by the X-ray temporal pulse width of  $\sim 100$  ps does not affect the time constant significantly in the investigated time range.

In summary, we determined accurate structural and kinetic information in the halogen elimination reactions in the solution-phase by using TXD. The transient structure of  $\cdot\text{CF}_2\text{CF}_2\text{I}$  in the photoinduced elimination reaction is determined to be a classical mixture whereas  $\cdot\text{CH}_2\text{CH}_2\text{I}$  is bridged. Compared with the gas-phase reaction whose structural dynamics was revealed by ultrafast gas electron diffraction, the secondary dissociation of  $\cdot\text{CF}_2\text{CF}_2\text{I}$  into  $\text{C}_2\text{F}_4$  and  $\text{I}$  is slowed down by a factor of 6 in methanol solution.

**Acknowledgment.** This work was supported by the Creative Research Initiatives (Center for Time-Resolved Diffraction) of MOST/KOSEF and the EU grant FLASH(FP6-503641).

## References

- (1) (a) Ihee, H.; Lorenc, M.; Kim, T. K.; Kong, Q. Y.; Cammarata, M.; Lee, J. H.; Bratos, M.; Wulff, M. *Science* **2005**, *309*, 1223–1227. (b) Kim, T. K.; Lorenc, M.; Lee, J. H.; Russo, M. L.; Kim, J.; Cammarata, M.; Kong, Q.; Noel, S.; Plech, A.; Wulff, M.; Ihee, H. *Proc. Natl. Acad. Sci. U.S.A.* **2006**, *25*, 9410–9415. (c) Lee, J. H.; Kim, K. H.; Kim, T. K.; Lee, Y.; Ihee, H. *J. Chem. Phys.* **2006**, *125*, 174504. (d) Reis, D. A.; Lindenberg, A. M. *Top. Appl. Phys.* **2007**, *108*, 371–422. (e) Lee, J. H.; Kim, J.; Cammarata, M.; Kong, Q.; Kim, K. H.; Choi, J.; Kim, T. K.; Wulff, M.; Ihee, H. *Angew. Chem., Int. Ed.* **2008**, *47*, 1047–1050.
- (2) (a) Zhong, D. P.; Ahmad, S.; Zewail, A. H. *J. Am. Chem. Soc.* **1997**, *119*, 5978–5979. (b) Rasmusson, M.; Taenovskiy, A. N.; Pascher, T.; Sundstrom, V.; Akesson, E. *J. Phys. Chem. A* **2002**, *106*, 7090–7098. (c) Khundkar, L. R.; Zewail, A. H. *J. Chem. Phys.* **1990**, *92*, 231–242.
- (3) (a) *Free Radicals in Organic Chemistry*; Fossey, J., Lefort, D., Sorba, J., Eds.; John Wiley & Sons: New York, 1995. (b) Ihee, H.; Zewail, A. H.; Goddard, W. A., III *J. Phys. Chem. A* **1999**, *103*, 6638–6649. (c) Skell, P. S.; Tuleen, D. L.; Readio, J. *J. Am. Chem. Soc.* **1963**, *85*, 2849–2850. (d) Ihee, H.; Kua, J.; Goddard, W. A., III; Zewail, A. H. *J. Phys. Chem. A* **2001**, *105*, 3623–3632.
- (4) (a) Ihee, H.; Lobastov, V. A.; Gomez, U.; Goodson, B. M.; Srinivasan, R.; Ruan, C.-Y.; Zewail, A. H. *Science* **2001**, *291*, 458–462. (b) Cao, J.; Ihee, H.; Zewail, A. H. *Proc. Natl. Acad. Sci. U.S.A.* **1999**, *96*, 338–342.
- (5) Elles, C. G.; Crim, F. F. *Annu. Rev. Phys. Chem.* **2006**, *57*, 273–302.
- (6) Cammarata, M.; Lorenc, M.; Kim, T. K.; Lee, J. H.; Kong, Q. Y.; Pontecorvo, E.; Russo, M. L.; Schiro, G.; Cupane, A.; Wulff, M.; Ihee, H. *J. Chem. Phys.* **2006**, *124*, 124504.
- (7) Kong, Q.; Kim, J.; Lorenc, M.; Kim, T. K.; Ihee, H.; Wulff, M. *J. Phys. Chem. A* **2005**, *109*, 10451–10458.
- (8) Aditya, S.; Willard, J. E. *J. Am. Chem. Soc.* **1957**, *79*, 2680–2681.

JA710267U